International Journal of Pharmaceutics 431 (2012) 204–209

Contents lists available at SciVerse ScienceDirect

International Journal of Pharmaceutics

journal homepage: www.elsevier.com/locate/ijpharm

Pharmaceutical Nanotechnology

Photodynamic therapy using glycol chitosan grafted fullerenes

Dong Sup Kwag[a], Nam Muk Oh[a], Young Taik Oh[b], Kyung Taek Oh[c], Yu Seok Youn[d], Eun Seong Lee[a,*]

[a] Division of Biotechnology, The Catholic University of Korea, 43-1 Yeokgok 2-dong, Wonmi-gu, Bucheon-si, Gyeonggi-do 420-743, Republic of Korea
[b] Department of Diagnostic Radiology, Yonsei University College of Medicine, 134 Shinchon-dong, Seodaemun-gu, Seoul 120-752, Republic of Korea
[c] College of Pharmacy, Chung-Ang University, 221 Heukseok dong, Dongjak-gu, Seoul 155-756, Republic of Korea
[d] College of Pharmacy, Sungkyunkwan University, 300 Chonchon-dong, Jangan-gu, Suwon-si, Gyeonggi-do 440-746, Republic of Korea

ARTICLE INFO

Article history:
Received 19 March 2012
Received in revised form 9 April 2012
Accepted 10 April 2012
Available online 17 April 2012

Keywords:
Fullerene conjugates
Glycol chitosan
Photodynamic therapy

ABSTRACT

Glycol chitosan (GC)-grafted fullerene (GC-*g*-C_{60}) conjugates were developed for use in photodynamic therapy of tumor cells. GC-*g*-C_{60} was synthesized in anhydrous benzene/dimethylsulfoxide (DMSO) co-solvent *via* the chemical conjugation of free amine groups of GC to C=C double bonds of C_{60}. The GC-*g*-C_{60} with 5×10^{-4} C_{60} molecules per one repeating unit of GC was soluble in water. As C_{60} molecules conjugated to GC increased to 0.16 molecules per one repeating unit of GC, GC-*g*-C_{60} started to form supramolecular assemblies (~30 nm) stabilized in phosphate buffer saline (PBS, 150 mM, pH 7.4). Upon 670 nm light illumination, photo-responsive properties of GC-*g*-C_{60} allowed tremendous singlet oxygen generation in tumor cells for super phototoxicity. GC-*g*-C_{60} also showed highly increased tumor accumulation ability for *in vivo* tumor of KB tumor-bearing nude mice. It is expected that our GC-*g*-C_{60} conjugate may be a good candidate for *in vivo* photodynamic therapy in various malignant tumor cells.

1. Introduction

Fullerene (C_{60}) is a soccer-ball-shaped truncated icosahedron with 12 pentagons (due to C_5—C_5 single bonds) and 20 hexagons (C_5—C_6 double bonds) (Mintmire, 1996; Bosi et al., 2003). Since the remarkable discovery of C_{60} in 1985, significant advances have been made in the development of modified fullerenes by exohedral derivatization using additional chemicals, polymers, proteins, antibodies, and genetic vectors (Bosi et al., 2003; Wei et al., 2010; Zhu et al., 2008; Hahn et al., 2007; Nakamura and Isobe, 2003). One of the most distinct features of these exohedral fullerenes is that their functionality that can be applied as antitumoral, antibacterial, antiviral, antioxidant, and diagnostic agents (Mintmire, 1996; Bosi et al., 2003; Wei et al., 2010). In particular, fullerenes's potential as a drug material for photodynamic therapy has been applied to improve chemo-therapeutic efficacy against tumor cells (Chen et al., 2005). It has been well-established that fullerenes are a potent photo-sensitizer that readily transfers the exited energy to oxygen molecules, resulting in reactive oxygen species (ROS) production (Anton et al., 1996). The photodynamic effect from the light-sensitization of fullerenes is the key contributor for the their photodynamic applications in therapy. Recent trials in fullerene design for photodynamic antitumor therapy have been directed towards the development of water-soluble fullerenes or nano-sized fullerene colloids to target tumor cells (Tabata and Ikada, 1999). However, even in the case of the sophistically designed exohedral fullerenes, there has been a lack of progress in their pharmaceutical approaches as part of drug discovery, drug delivery, and disease diagnostics (Anton et al., 1996; Diener et al., 2007; Tabata and Ikada, 1999).

Here, we describe a facile synthesis of fullerene derivatives for photodynamic therapy. We utilized a chemical modification strategy by chemically conjugating the free amine groups of glycol chitosan (GC) to the C=C double bonds of fullerene (Fig. 1a). GC-grafted fullerenes were easily synthesized in anhydrous benzene/dimethylsulfoixde (DMSO) co-solvent at room temperature. GC, a derivative of chitosan and water soluble over a large pH range, is known to posses potentially biocompatible and biodegradable properties (Oh et al., 2010; Park et al., 2011; Baik et al., 2011; Lee et al., 2010, 2011a). Hydrophobically modified GC nanoparticles has been shown to be able to enclose water-insoluble drugs and to decrease non-specific interactions with biological components during systemic circulation (Park et al., 2006; Nam et al., 2009). GC-grafted fullerenes (GC-*g*-C_{60}) are expected to provide good stability (or dispersion) in serum and high photodynamic activity against tumor cells.

2. Materials and methods

2.1. Materials

Fullerene (C_{60}) was purchased from NanoLab Inc. (Waltham, MA, USA). Glycol chitosan (GC, Mw = 500 kDa), dimethylsulfoxide (DMSO), triethylamine (TEA), anhydrous benzene, sodium

* Corresponding author. Tel.: +82 2 2164 4921; fax: +82 2 2164 4865.
E-mail address: eslee@catholic.ac.kr (E.S. Lee).

0378-5173/$ – see front matter © 2012 Elsevier B.V. All rights reserved.
http://dx.doi.org/10.1016/j.ijpharm.2012.04.038

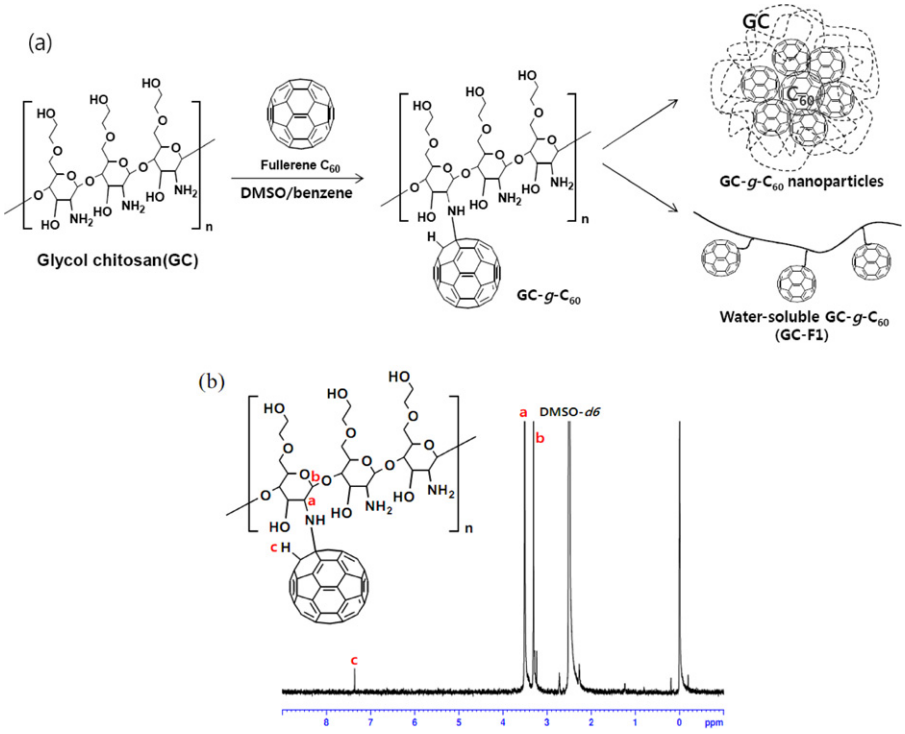

Fig. 1. GC-*g*-C_{60} preparation. (a) Synthesis scheme and concept of purposed GC-*g*-C_{60} conjugates. (b) ^{1}H NMR peak of GC-*g*-C_{60} conjugates.

borate ($Na_2B_4O_7$), 9,10-dimethylanthracene (DMA), N-N′-dicyclohexylcarbodiimide (DCC), and N-hydroxysuccinimide (NHS) were purchased from Sigma–Aldrich (St. Louis, MO, USA). RPMI-1640, fetal bovine serum (FBS), penicillin, and streptomycin were purchased from Welgene, Inc. (Seoul, South Korea). Chlorin e6 (Ce6) was purchased from Frontier Scientific, Inc. (Logan, UT, USA). The Cell Counting Kit-8 was obtained from Dojindo Molecular Technologies Inc. (Kumamoto, Japan). The Annexin V-RITC fluorescence microscopy kit was purchased from BD Pharmingen™ (USA).

2.2. GC-g-C_{60} synthesis

C_{60} (0.35–71 mg) and GC (100 mg) were reacted in anhydrous benzene (10 ml)/DMSO (10 ml) co-solvent containing TEA (1 ml) at room temperature for 2 days (Fig. 1a). After the reaction, benzene was removed using a rotary evaporator and the resulting solution was added to a pre-swollen dialysis membrane tube (Spectra/Por® MWCO 15 K) and was dialyzed against borate buffer (pH 7.4) solution to remove non-reacted chemicals. The solution withdrawn from a dialysis membrane tube was lyophilized after freeze-drying for 2 days. The conjugation of C_{60} to GC was estimated from ^{1}H NMR (DMSO-d_6 with TMS) from the peaks from δ 7.26 ppm [—C**H** in C_{60} part of GC-*g*-C_{60}] and δ 3.50 ppm [—C**H**$_2$ in GC] (Fig. 1b).

2.3. Characterization of GC-g-C_{60}

The particle size distribution of GC-*g*-C_{60} (0.1 mg/ml) was measured with a Zetasizer 3000 instrument (Malvern Instruments, Westborough, MA, USA) equipped with a He–Ne laser beam at a wavelength of 632.8 nm and a fixed scattering angle of 90°. The morphology of GC-*g*-C_{60} (10 μg/ml) was confirmed using a field emission scanning electron microscopy (FE-SEM, Hitachi s-4800, Tokyo, Japan). The UV/visible spectra of GC-*g*-C_{60} conjugates (0.05 mg/ml) and free C_{60} (0.05 mg/ml) in benzene/DMSO (50/50 vol.%) co-solvent were monitored at 300–800 nm.

The generation of singlet oxygen of GC-*g*-C_{60} (0.1 mg/ml) was confirmed using 9,10-dimethylanthracene (DMA) (Park et al., 2011, 2012; Oh et al., 2012). DMA (20 mmol) was mixed with GC-*g*-C_{60} (0.1 mg/ml) in PBS (150 mM, pH 7.4). The solution was illuminated at a light intensity of 100 mW/cm^2 using a 670 nm laser source for 10 min. When the DMA fluorescence intensity (measured using a Shimadzu RF-5301PC spectrofluorometer at λ_{ex} 360 nm and λ_{em} 380–550 nm) reached a plateau after 1 h, the change in DMA fluorescence intensity ($F_f - F_s$) was plotted after subtracting each sample fluorescence intensity (F_s) from the full DMA fluorescence intensity (without GC-*g*-C_{60} or C_{60}, indicating no singlet oxygen, F_f) (Park et al., 2011, 2012; Oh et al., 2012). All data were obtained by using the slit-width of the excitation and the emission of the spectrofluorometer at 5 nm.

2.4. In vitro phototoxicity

Human nasopharyngeal epidermal carcinoma KB cells were maintained in RPMI-1640 medium with 2 m L-glutamine, 1% penicillin–streptomycin, and 10% FBS in a humidified standard incubator with a 5% CO_2 atmosphere at 37 °C. Prior to testing, cells (1×10^5 cells/ml), grown as a monolayer, were harvested *via* trypsinization using a 0.25% (w/v) trypsin/0.03% (w/v) EDTA solution. KB cells suspended in RPMI-1640 medium were seeded onto well plates and cultured for 24 h prior to *in vitro* cell testing (Park et al., 2011, 2012; Oh et al., 2012).

Phototoxicity of GC-*g*-C_{60} with light illumination was tested in KB tumor cells (Park et al., 2011, 2012; Oh et al., 2012). GC-*g*-C_{60} or free C_{60} dispersed in RPMI-1640 medium was administered to cells plated in 96-well plates. The cells were incubated with each sample for 4 h and then washed three times with PBS (pH 7.4). The cells were illuminated at a light intensity of 100 mW/cm^2 using a 670 nm laser source for 10 min and then further incubated for 6 h. Cell viability was determined using a Cell Counting Kit-8 (CCK-8 assay). In addition, the cell viability test of KB cells treated with GC-*g*-C_{60} without light illumination was conducted to estimate the

Table 1
Characterization of GC-*g*-C_{60}.

Compound	Feeding C_{60} molecules per one repeating unit of GC	Conjugated C_{60} molecules per one repeating unit of GC
GC-F1	0.001	5×10^{-4}
GC-F2	0.005	2×10^{-3}
GC-F3	0.01	2×10^{-3}
GC-F4	0.05	2×10^{-2}
GC-F5	0.2	0.16

original toxicity of GC-*g*-C_{60}. The cells were incubated for 24 h with GC-*g*-C_{60} and then evaluated *via* a CCK-8 assay.

Tumor cellular apoptosis was also visualized using an Annexin V-RITC fluorescence microscopy kit (Park et al., 2011, 2012; Oh et al., 2012). KB tumor cells were incubated with each sample (equivalent C_{60} 5 μg/ml) for 4 h and then washed three times with PBS (pH 7.4). The tumor cells illuminated at a light intensity of 100 mW/cm^2 using a 670 nm laser source for 10 min were washed twice with PBS and stained with 1 ml of Annexin V-RITC (10 wt.%) for 15 min at room temperature. After staining, the tumor cells were washed twice with PBS and then fixed using 3.7% formaldehyde in PBS. A cover slip was mounted on a microscope slide with a drop of anti-fade mounting media (5% *N*-propyl galate, 47.5% glycerol and 47.5% Tris–HCl, pH 8.4) to reduce fluorescence photo-bleaching. Cellular apoptosis was visualized using a fluorescence microscope (at λ_{ex} 570 nm and λ_{em} 595 nm, E-SCOPE 1500F) (Park et al., 2011, 2012; Oh et al., 2012).

2.5. Animal care

In vivo studies were conducted with 4 to 6-week old female nude mice (BALB/c, nu/nu mice, Institute of Medical Science, Tokyo, Japan). Mice were maintained under the guidelines of an approved protocol from the Institutional Animal Care and Use Committee (IACUC) of the Catholic University of Korea (Republic of Korea).

2.6. In vivo fluorescence imaging

Before the animal test, fluorescent dye (Ce6) (1 mg) pre-activated with DCC (2 mg) and NHS (2 mg) in DMSO (1 ml) was tagged to GC-*g*-C_{60} (100 mg) in DMSO (10 ml) at room temperature and was stirred for 4 h. The solution was filtrated to remove dicyclohexylurea (DCU) and then dialyzed with a dialysis membrane bag (Spectra/Por® MWCO 1 K), followed by lyophilization.

For the *in vivo* animal experiments, KB tumor cells were introduced into female nude mice *via* subcutaneous injection of 1×10^4 cells suspended in PBS pH 7.4 (ion strength: 0.15) medium. When the tumor volume reached about 30 mm^3, Ce6-tagged GC-*g*-C_{60} conjugates (equivalent C_{60} 10 mg/kg body) or PBS solution alone (ionic strength = 0.15, pH 7.4) was injected intravenously into tumor-bearing nude mice through the tail vein. A 12-bit CCD camera (Image Station 4000 MM; Kodak, Rochester, NY, USA) prepared with a special C-mount lens and a long wave emission filter (600–700 nm; Omega Optical, Brattleboro, VT, USA) were used to capture live fluorescence images of the nude mice (Park et al., 2011, 2012; Oh et al., 2012; Lee et al., 2011a, 2011b).

3. Results and discussion

3.1. Characterization of GC-g-C_{60}

GC-*g*-C_{60} was prepared through the chemical reaction between free amine groups of GC and C=C double bonds of C_{60} (Fig. 1a). The degree of substitution (DS, defined as the number of C_{60} molecules

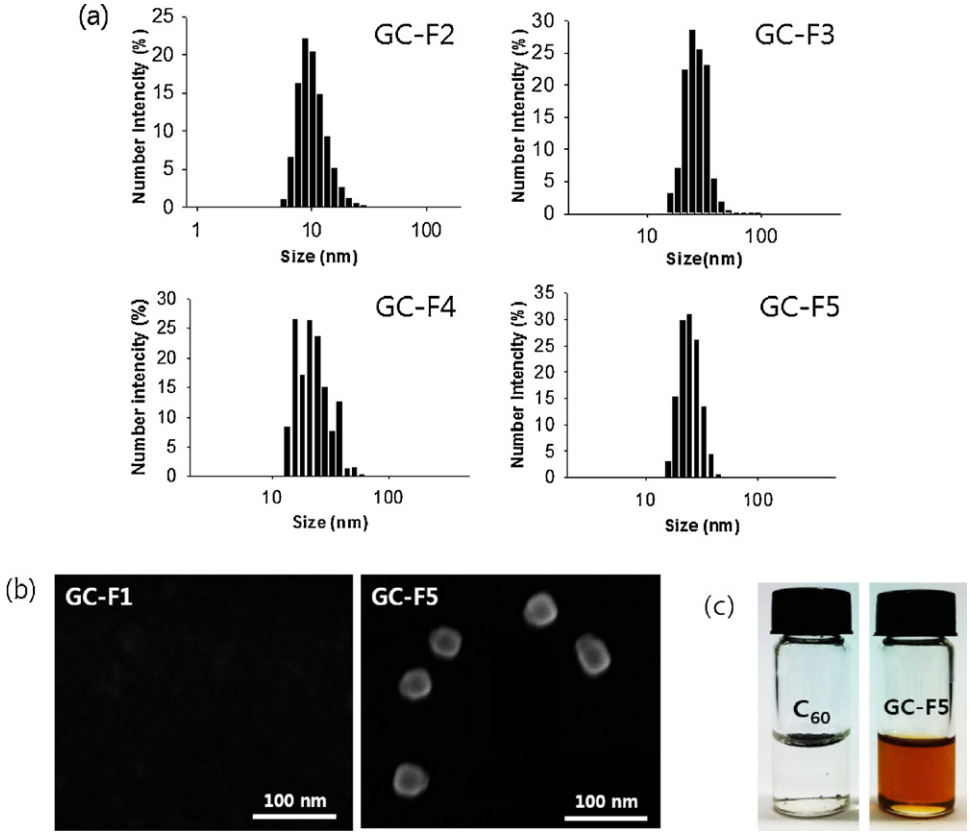

Fig. 2. Characterization of GC-*g*-C_{60}. (a) Particle size distribution of GC-*g*-C_{60} conjugates: GC-F2, GC-F3, GC-F4, and GC-F5. (b) FE-SEM images of GC-F1 and GC-F5. (c) Optical image of free C_{60} or GC-F5 dispersed in PBS solution (150 mM, pH 7.4, 1 mg/ml).

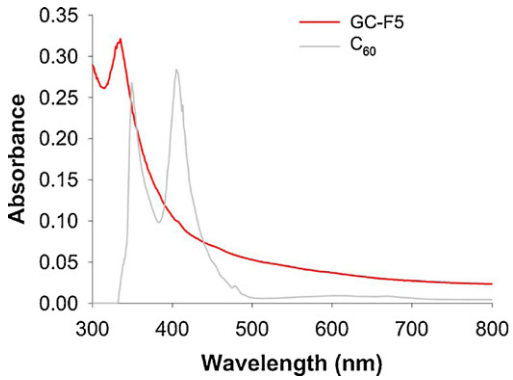

Fig. 3. UV/visible spectrum of GC-F5 or free C_{60} in DMSO/benzene co-solvent. The concentrations of all samples were fixed to 0.05 mg/ml.

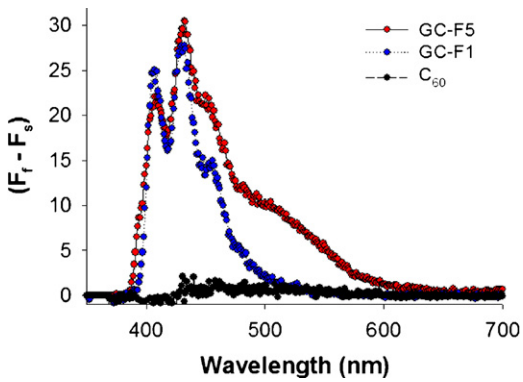

Fig. 4. The generation of singlet oxygen of GC-*g*-C_{60} conjugates (equivalent C_{60} 0.1 mg/ml) in PBS (150 mM, pH 7.4).

per one repeating unit of GC) ranged from 5×10^{-4} to 0.16 (Table 1), as determined by the ^{1}H NMR (DMSO-d_6 with TMS) peaks from δ 7.26 ppm [—C**H** in C_{60} part of GC-*g*-C_{60}] to δ 3.50 ppm [—C**H**$_2$ in GC] (Fig. 1b). The conjugation of C_{60} is considered to confer photodynamic activity to the polysaccharidic conjugate and a rich lipophilicity for self-organized architecture (Park et al., 2011, 2012; Oh et al., 2012) of the polysaccharidic conjugate. As C_{60} molecules conjugated to GC increased from 5×10^{-4} to 0.16 molecules per one repeating unit of GC, GC-*g*-C_{60} was self-organized in PBS (150 mM, pH 7.4), forming nanoparticles (Fig. 1a). As shown in Fig. 2a, the average particle size of GC-*g*-C_{60} nanoparticles (prepared using GC-F2, GC-F3, GC-F4 or GC-F5 in Table 1) was approximately 10–23 nm. These GC-*g*-C_{60} nanoparticles were stable more than one month under optimal conditions without any precipitation. Over this time, the particle size and the transmittance of GC-*g*-C_{60} nanoparticles did not change (data not shown). The morphological images obtained from FE-SEM revealed nearly spherical GC-*g*-C_{60} nanoparticles (GC-F5) at pH 7.4 (Fig. 2b). We detected no difference in the shape of GC-F2, GC-F3, GC-F4, and GC-F5 nanoparticles (data not shown). However, GC-*g*-C_{60} with 5×10^{-4} C_{60} molecules per one repeating unit of GC (GC-F1 in Table 1) was clearly soluble in water (Fig. 1a), resulting in no detection from the FE-SEM image (Fig. 2b). In addition, Fig. 2c demonstrated good colloidal stability of GC-F5 nanoparticles due to the hydrodynamic GC cloud surrounding C_{60} molecules, while free C_{60} molecules rapidly aggregated in 5 min and floated in PBS solution due to their low density.

3.2. *Light-sensitive GC-g-C_{60}*

The UV/visible spectrum of GC-*g*-C_{60} conjugate (0.05 mg/ml) showed distinct absorption bands in the 300–800 nm range due to the presence of GC and C_{60} (Fig. 3). GC-*g*-C_{60} conjugates allowed

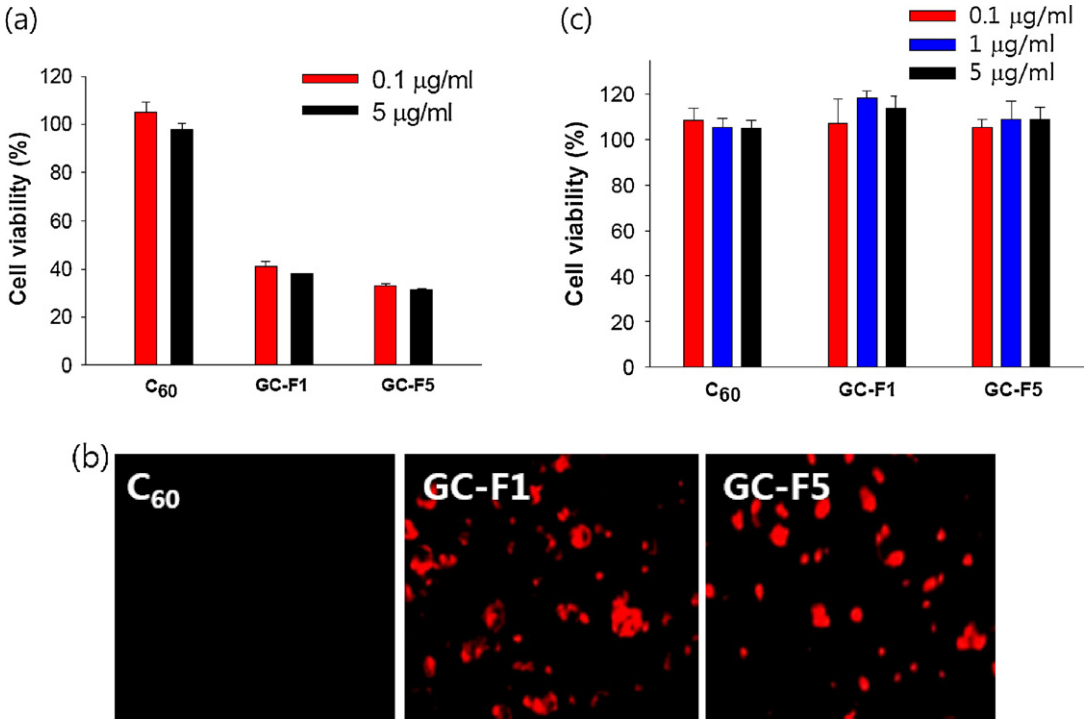

Fig. 5. *In vitro* antitumor effect of GC-*g*-C_{60}. (a) Phototoxicities were determined using a CCK-8 assay in KB cells treat with free C_{60} (0.1–5 μg/ml), GC-F1 (equivalent C_{60} 0.1–5 μg/ml), and GC-F5 (equivalent C_{60} 0.1–5 μg/ml) under light illumination ($n = 7$). (b) Fluorescence images of KB tumor cells treated with free C_{60} (1 μg/ml), GC-F1 (equivalent C_{60} 1 μg/ml), and GC-F5 (equivalent C_{60} 1 μg/ml) for 4 h with light illumination. Annexin V-RITC staining (red) depicts apoptotic cells. (c) Cell viabilities of KB cells treated with free C_{60} (0.1–5 μg/ml), GC-F1 (equivalent C_{60} 0.1–5 μg/ml), and GC-F5 (equivalent C_{60} 0.1–5 μg/ml) without light illumination for 24 h ($n = 7$). (For interpretation of the references to color in this figure legend, the reader is referred to the web version of this article.)

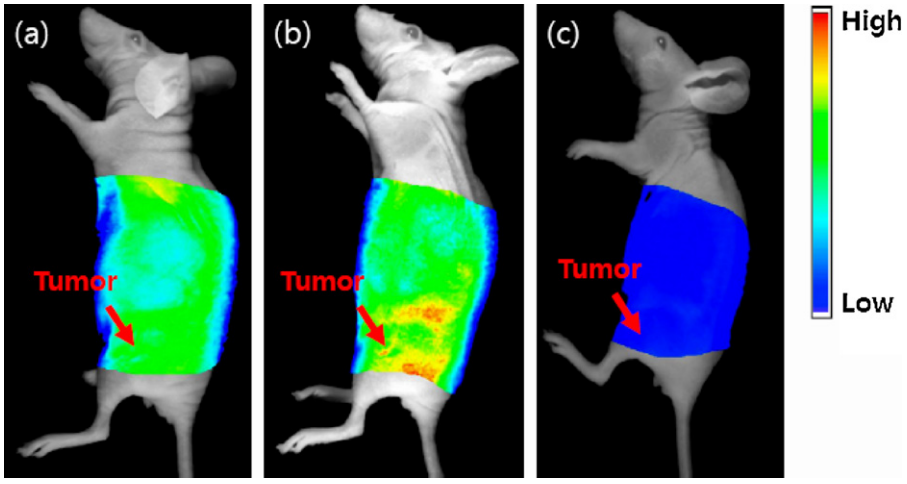

Fig. 6. *In vivo* non-invasive fluorescent imaging of nude mice harboring KB tumors. GC-F1 (equivalent C_{60} 10 mg/kg body), GC-F5 (equivalent C_{60} 10 mg/kg body), or only PBS (ion strength = 0.15, pH 7.4) was intravenously injected into nude mice and fluorescent images were obtained after 4 h.

a strong optical absorption at 328 nm, different with a strong optical absorption at 408 nm of free C_{60} molecules. The introduction of GC to C_{60} molecules seemed to affect light-sensitization of C_{60} molecules. Interestingly, the improved light absorption of GC-*g*-C_{60} at 670 nm in the near-infrared (NIR) region is expected to provide increased excited energy to oxygen molecules to generate reactive oxygen species (ROS) such as singlet oxygen (Anton et al., 1996; Bosi et al., 2003; Wei et al., 2010; Zhu et al., 2008; Hahn et al., 2007; Nakamura and Isobe, 2003).

Fig. 4 presents the singlet oxygen generation from GC-*g*-C_{60} conjugate during light illumination. For this test, we utilized 9,10-dimethylanthracene (DMA) as an extremely fast chemical trap for singlet oxygen (Park et al., 2011, 2012; Oh et al., 2012). Fluorescent DMA reacts selectively with singlet oxygen to form the endoperoxide (Gomes et al., 2005), thus causing the reduction in the fluorescence of DMA. Herein, we illuminated GC-*g*-C_{60} conjugates (equivalent C_{60} 0.1 mg/ml) or free C_{60} molecules (0.1 mg/ml) for 10 min at a light intensity of 100 mW/cm^2 using a 670 nm laser source. The changes in DMA fluorescence intensity were monitored in order to confirm singlet oxygen generation from GC-*g*-C_{60} conjugates or free C_{60}. The change in DMA fluorescence intensity ($F_f - F_s$) indicates the generation of substantially more singlet oxygen (Park et al., 2011, 2012; Oh et al., 2012). GC-*g*-C_{60} conjugates (GC-F1, GC-F5) stabilized in PBS (150 mM, pH 7.4) generated higher singlet oxygen than C_{60} molecules aggregated in PBS.

3.3. Antitumoral activity of GC-g-C_{60}

Fig. 5 shows the *in vitro* anticancer therapeutic efficiency of GC-*g*-C_{60}. The photodynamic cell abelation of GC-*g*-C_{60} under light illumination was tested for human cervical carcinoma KB tumor cells. GC-*g*-C_{60} conjugates or free C_{60} dispersed in RPMI-1640 medium was administered to cells plated in 96-well plates. The cells were incubated with each sample for 4 h and then washed three times with PBS (pH 7.4). The cells were illuminated at a light intensity of 100 mW/cm^2 using a 670 nm laser source for 10 min and then further incubated for 6 h. Upon these procedures, GC-F5 or GC-F1 led to relatively high levels of KB cell death (Fig. 5a), reflecting highly improved photodynamic cell damage by tremendous singlet oxygen generation from GC-F5 or GC-F1. Annexin V-RITC staining (Park et al., 2011, 2012; Lee et al., 2011b) showed an extensive apoptotic cell population induced by GC-F1 or GC-F5, corresponding to a strong red fluorescence in KB tumor cells (Fig. 5b). However, free C_{60} caused less phototoxicity of KB tumor cells. It is interesting to note that GC-*g*-C_{60} conjugates or free C_{60} prior to light illumination were not cytotoxic (Fig. 5c).

In an attempt to further evaluate the potential of GC-*g*-C_{60} as a photosensitizer for tumor therapy, *in vivo* efficacy for BALB/c nu/nu female mice harboring KB tumors was assessed. A fluorescent dye (Chlorin e6: Ce6) was coupled to GC-*g*-C_{60} for *in vivo* fluorescent imaging (Park et al., 2011, 2012; Oh et al., 2012; Lee et al., 2011a, 2011b). A 12-bit CCD camera (Image Station 4000 MM; Kodak) prepared using a special lens and a long wave emission filter (600–700 nm) was used to obtain fluorescence images of nude mice (Park et al., 2011, 2012; Oh et al., 2012; Lee et al., 2011a, 2011b). *In vivo* fluorescent images of KB tumor-bearing nude mice were obtained at 4 h after the intravenous injection of Ce6-labeled GC-*g*-C_{60} conjugates (GC-F1 or GC-F5) or only PBS through the tail veins of nude mice. We were able to obtain high-resolution fluorescent images of the tumor site with small volume (~30 mm^3) from the nude mice injected with GC-F5 (Fig. 6b), comparable to the rapid clearance observed with an injection with water-soluble GC-F1 (Fig. 6a) or the background condition with PBS solution (Fig. 6c). The high accumulation of GC-F5 in the tumor site can be explained by GC-F5 extravasation from the tumor vasculature due to the enhanced permeability and retention (EPR) effect (Maeda and Matsumura, 2011). It is reasonable to assume that the efficient delivery of C_{60} into target tumor site will enable a local high dose therapy that maximizes its therapeutic activity at target site. To substantiate our findings of its potential, further investigations such as *in vivo* tumor inhibition test will be required.

4. Conclusion

GC-*g*-C_{60} conjugates exhibited an advanced capacity for C_{60} solubilization, the photodynamic tumor cell ablation, and to carry C_{60} in the body. These qualities of GC-*g*-C_{60} are anticipated to increase the utility of C_{60} for photodynamic antitumor therapy. We conclude that GC-*g*-C_{60} conjugates hold great promise for use in the selective delivery of anticancer drugs to tumor cells *in vivo*.

Acknowledgements

This work was financially supported by a grant from the Korean Health Technology R&D Project, Ministry of Health & Welfare (No.

A111291), by a research grant funded by the Gyeonggi Regional Research Center (GRRC), and by the Basic Science Research Program through the National Research Foundation of Korea (NRF) funded by the Ministry of Education, Science, and Technology (No. 2011-0004766).

References

Anton, W.J., Stephen, R.W., David, I., 1996. Biological applications of fullerenes. Bioorg. Med. Chem. 4, 767–779.

Baik, H.J., Oh, N.M., Oh, Y.T., Yoo, N.Y., Park, S.Y., Oh, K.T., Youn, Y.S., Lee, E.S., 2011. 3-Diethylaminopropyl-bearing glycol chitosan as a protein drug carrier. Colloids Surf. B: Biointerfaces 84, 585–590.

Bosi, S., Da Ros, T., Spalluto, G., Prato, M., 2003. Fullerene derivatives: an attractive tool for biological applications. Eur. J. Med. Chem. 38, 913–923.

Chen, C., Xing, G., Wang, J., Zhao, Y., Li, B., Tang, J., Jia, G., Wang, T., Sun, J., Xing, L., Yuan, H., Gao, Y., Meng, H., Chen, Z., Zhao, F., Chai, Z., Fang, X., 2005. Multihydroxylated $[Gd@C_{82}(OH)_{22}]_n$ nanoparticles: antineoplastic activity of high efficiency and low toxicity. Nano Lett. 5, 2050–2057.

Gomes, A., Fernandes, E., Lima, J.L.F.C., 2005. Fluorescence probes used for detection of reactive oxygen species. J. Biochem. Biophys. Methods 65, 45–80.

Hahn, U., Gegout, A., Duhayon, C., Coppel, Y., Saquet, A., Nierengarten, J.F., 2007. Self-assembly of fullerene-rich nanostructures with a stannoxane core. Chem. Commun. 5, 516–518.

Lee, B.R., Oh, K.T., Baik, H.J., Youn, Y.S., Lee, E.S., 2010. A charge-switched nano-sized polymeric carrier for protein delivery. Int. J. Pharm. 392, 78–82.

Lee, B.R., Oh, K.T., Oh, Y.T., Baik, H.J., Park, S.Y., Youn, Y.S., Lee, E.S., 2011a. A novel pH-responsive polysaccharidic ionic complex for proapoptotic (KLAKLAK)2 peptide delivery. Chem. Commun. 47, 3852–3854.

Lee, W.R., Oh, K.T., Park, S.Y., Yoo, N.Y., Ahn, Y.S., Lee, D.H., Youn, Y.S., Lee, D.K., Cha, K.H., Lee, E.S., 2011b. Magnetic levitating polymeric nano/microparticular substrates for three-dimensional tumor cell culture. Colloids Surf. B: Biointerfaces 85, 379–384.

Diener, M.D., Alford, J.M., Kennel, S.J., Mirazdeh, S., 2007. $(212)Pb@C_{60}$ and its water-soluble derivatives: synthesis, stability, and suitability for radioimmunotherapy. J. Am. Chem. Soc. 129, 5131–5138.

Maeda, H., Matsumura, Y., 2011. EPR effect based drug design and clinical outlook for enhanced cancer chemotherapy. Adv. Drug Deliv. Rev. 63, 129–130.

Mintmire, J.W., 1996. Fullerene formation and annealing. Science 272, 45–46.

Nakamura, E., Isobe, H., 2003. Functionalized fullerenes in water. The first 10 years of their chemistry, biology, and nanoscience. Acc. Chem. Res. 36, 807–815.

Nam, H.Y., Kwon, S.M., Chung, H., Lee, S.Y., Kwon, S.H., Jeon, H., Kim, Y., Park, J.H., Kim, J., Her, S., Oh, Y.K., Kwon, I.C., Kim, K., Jeong, S.Y., 2009. Cellular uptake mechanism and intracellular fate of hydrophobically modified glycol chitosan nanoparticles. J. Control. Release 135, 259–267.

Oh, N.M., Kwag, D.S., Park, S.Y., Oh, K.T., Youn, Y.S., Lee, E.S., 2012. Electrostatic charge conversion processes in engineered tumor-identifying polypeptides for targeted chemotherapy. Biomaterials 33, 1884–1893.

Oh, N.M., Oh, K.T., Baik, H.J., Lee, B.R., Lee, A.H., Youn, Y.S., Lee, E.S., 2010. A self-organized 3-diethylaminopropyl-bearing glycol chitosan nanogel for tumor acidic pH targeting: evaluation. Colloids Surf. B: Biointerfaces 78, 120–126.

Park, J.H., Kwon, S., Lee, M., Chung, H., Kim, J.H., Kim, Y.S., Park, R.W., Kim, I.S., Seo, S.B., Kwon, I.C., Jeong, S.Y., 2006. Self-assembled nanoparticles based on glycol chitosan bearing hydrophobic moieties as carriers for doxorubicin: in vivo biodistribution and anti-tumor activity. Biomaterials 27, 119–126.

Park, S.Y., Baik, H.J., Oh, Y.T., Oh, K.T., Youn, Y.S., Lee, E.S., 2011. A smart polysaccharide/drug conjugate for photodynamic therapy. Angew. Chem. Int. Ed. Engl. 50, 1644–1647.

Park, S.Y., Oh, N.M., Oh, Y.T., Oh, K.T., Youn, Y.S., Lee, E.S., 2012. Artificial photosensitizer drug network for mitochondria-selective photodynamic therapy. Chem. Commun. 48, 2522–2524.

Tabata, Y., Ikada, Y., 1999. Biological functions of fullerene. Pure Appl. Chem. 71, 2047–2053.

Wei, P., Zhang, L., Lu, Y., Man, N., Wen, L., 2010. C_{60}(Nd) nanoparticles enhance chemotherapeutic susceptibility of cancer cells by modulation of autophagy. Nanotechnology 21, 495101.

Zhu, J., Ji, Z., Wang, J., Sun, R., Zhang, X., Gao, Y., Sun, H., Liu, Y., Wang, Z., Li, A., Ma, J., Wang, T., Jia, G., Gu, Y., 2008. Tumor-inhibitory effect and immunomodulatory activity of fullerol $C_{60}(OH)_x$. Small 4, 1168–1175.